

Effects of the symmetry energy slope on magnetized neutron stars

Luiz L. Lopes,^{1,*} César V. Flores,^{2,3,†} and Débora P. Menezes^{4,‡}

¹*Centro Federal de Educação Tecnológica de Minas Gerais Campus VIII, CEP 37.022-560, Varginha, Brazil*

²*Universidade Estadual da Região Tocantina do Maranhão, UEMASUL,*

Centro de Ciências Exatas, Naturais e Tecnológicas, Imperatriz, CEP 65901-480 Maranhão, Brazil

³*Universidade Federal do Maranhão, Programa de Pós-graduação em Física, 65080-805, São Luís, Maranhão, Brazil*

⁴*Depto de Física, CFM, Universidade Federal de Santa Catarina, Florianópolis, SC, CP:476, CEP 88.040-900, Brazil*

In this work, we study the effect of the symmetry slope on the observables of weakly and strongly magnetized neutron stars within the chaotic magnetic field approximation. We investigate the impact of the symmetry energy slope in the equation of state, as well as on the observables of neutron stars, by calculating their masses, radii, redshifts, tidal deformabilities, and fundamental-mode gravitational-wave frequencies.

I. INTRODUCTION

It is very well known that magnetic fields are of outstanding importance in the study of physical phenomena. Those magnetic fields range from 10^{-11} G (e.g. in the human brain) to 10^{18} G (e.g. in the early Universe and heavy-ion collisions). Other values include Earth's magnetic fields, which are of the order of 10^{-1} G, 50 G present in refrigerator magnets, 10^5 G in modern nuclear magnetic resonance equipment, and $10^{12} - 10^{13}$ G in the crust of neutron stars.

This article focuses on magnetars [1, 2], a special class of neutron stars with surface magnetic fields three orders of magnitude stronger than the ones present in standard neutron stars, i.e., up to 10^{15} G at their surface. Most of the known magnetars detected so far are isolated objects; i.e., they are not part of a binary system and manifest themselves as either transient X-ray sources, known as soft- γ repeaters, or persistent anomalous X-ray pulsars. At the moment, only thirty magnetars have been identified [3], but modern telescopes are a promise for more information. The NICER telescope has already detected two hot spots in the same hemisphere of an ordinary pulsar, suggesting a magnetic field configuration more complex than perfectly symmetric dipoles. It is important to emphasize that the magnetars detected so far are isolated objects, but there is no reason to believe that binary systems do not exist.

Any realistic neutron star model must be able to fulfill some experimental and observational constraints coming from both terrestrial nuclear experiments and neutron stars' observations. To describe the interior of a neutron star, we use an extended version of quantum hadrodynamics (QHD) [4] with the L3 $\omega\rho$ parametrization [5]. This parameterization is capable of fulfilling five phenomenological constraints at the saturation point: the saturation point itself (n_0), the incompressibility, (K), the symmetry energy (S_0), the binding energy per nucleon (B/A), and the nucleon effective mass at the saturation density (M^*/M), as discussed in two extensive review papers [6, 7]. A sixth parameter, the symmetry energy slope (L) is left as a free parameter, so that we can investigate how it affects the equation of state (EOS) and the neutron stars' macroscopic properties for both weak and strong magnetized stellar matter.

From the astrophysical observation, we check what values of the slope and the influence of the magnetic field can fulfill the constraints related to the PSR J0740+6620, with a mass of $2.08 \pm 0.07 M_\odot$ and a radius in the range of $11.41 \text{ km} < R < 13.69 \text{ km}$ [8, 9] and the dimensionless tidal parameter of the canonical star, as pointed in ref. [10].

Intending to observe the effect of the symmetry slope on the observables of weakly and strongly magnetized neutron stars, we have computed their mass, radii, redshift, tidal deformability, and the gravitational wave frequency of the fundamental mode. At the end of the paper, we also add a small discussion related to the universal relations and compare our findings with those presented in the literature. We expect that future astronomical observables can help in the discrimination of these magnetized compact stars.

*Electronic address: llopes@cefetmg.br

†Electronic address: cezarovf@gmail.com

‡Electronic address: debora.p.m@ufsc.br

II. FORMALISM

To characterize the interactions between protons and neutrons under the influence of a background magnetic field, we use an extended version of the QHD Lagrangian. We also add leptons to account for the zero charge neutrality condition. After this physical considerations we can see that the total Lagrangian in the mean field approximation (MFA) reads [4, 11–13]:

$$\begin{aligned} \mathcal{L} = \sum_N \bar{\psi}_N & \left[\gamma^0 (i\partial_0 - g_{N\omega}\omega_0 - \frac{1}{2}g_{N\rho}\tau_3\rho_0) - \gamma^j (i\partial_j + e_N A_j) - M_N^* \right] \psi_N \\ & - \frac{1}{2}m_s^2\sigma_0^2 + \frac{1}{2}m_\omega^2\omega_0^2 + \frac{1}{2}m_\rho^2\rho_0^2 - \frac{1}{3}\kappa M_N(g_{Ns}\sigma_0)^3 - \frac{1}{4}\lambda(g_{Ns}\sigma_0)^4 \\ & + \Lambda_{\omega\rho}(g_{N\rho}^2g_{N\omega}^2\rho_0^2\omega_0^2) + \sum_l \bar{\psi}_l [(\gamma^\mu(i\partial_\mu - e_l A_\mu) - m_l)\psi_l], \end{aligned} \quad (1)$$

where ψ_N and ψ_l are the Dirac fields of the nucleons and leptons, respectively; the g 's are the Yukawa coupling constants that simulate the strong interaction; the $\gamma^\mu = (\gamma^0, \gamma^j)$ are the Dirac matrices; τ_3 is the third Pauli matrix; $M_N^* = M_N - g_{N\sigma}\sigma_0$ is the nucleon effective mass, with $M_N = 939$ MeV; $m_l = (m_e, m_\mu)$ are the masses of the leptons, 0.511 MeV and 105.6 MeV, respectively; κ and λ are coupling constants related to the σ -meson self interaction, needed to correct the value of the incompressibility [14], $\Lambda_{\omega\rho}$ is the coupling constant related to the non-linear interaction between the ρ and ω mesons, necessary to correct the value of the slope L [11], $A^\mu = (A^0, A^j)$ is the electromagnetic four-potential, and e_N and e_l are the electric charge of the nucleons and leptons respectively. The electric charge of neutrons (n), protons (p), and both leptons (l) is 0, $+e$, and $-e$, respectively.

By applying the Euler-Lagrange equations, we obtain the equations of motions and the nucleons and leptons energy eigenvalues, which at zero temperature are also their chemical potentials. For a constant magnetic field in the z direction, we have [15]:

$$\begin{aligned} E_n &= \sqrt{M_N^* + k^2} + g_{N\omega}\omega_0 - \frac{1}{2}g_{N\rho}\rho_0, \\ E_p &= \sqrt{M_N^* + k_z^2 + 2\nu|e|B} + g_{N\omega}\omega_0 + \frac{1}{2}g_{N\rho}\rho_0, \\ E_l &= \sqrt{m_l + k_z^2 + 2\nu|e|B}, \end{aligned} \quad (2)$$

where n refers to neutrons, p to protons, ν is a discrete parameter related to the Landau level (LL) and B is the magnetic field. The number densities of neutrons, protons, and leptons are:

$$\begin{aligned} n_n &= \frac{k_{Fn}^3}{3\pi^2}, \quad n_p = \frac{|e|B}{2\pi^2} \sum_\nu \eta(\nu) k_{zFp}, \\ n_l &= \frac{|e|B}{2\pi^2} \sum_\nu \eta(\nu) k_{zFl}, \end{aligned} \quad (3)$$

where the subscript F indicates Fermi momentum. The $\eta(\nu)$ is the degeneracy of the Landau level ν , which reads $\eta(\nu) = 1$ for $\nu = 0$ and $\eta(\nu) = 2$ for $\nu > 0$. The summation in ν in the above expressions runs up to ν_{max} , the largest integer value of ν for which the squared Fermi momenta of the particle is positive and it is defined below for protons and leptons:

$$\nu_{max(p)} = \frac{\mu_p^2 - M_N^{*2}}{2|e|B}, \quad \text{and} \quad \nu_{max(l)} = \frac{\mu_l^2 - m_l^{*2}}{2|e|B}. \quad (4)$$

To obtain stellar matter EOS, charge neutrality and chemical equilibrium conditions have to be enforced. The equation of state for baryons, leptons, and mesons is derived from statistical mechanics, as discussed in Refs. [12–17] and the references therein.

Now, since the magnetic field itself presents energy and pressure, we must explicitly take it into account in the EOS. However, while the energy density of the magnetic field is easily added, the contribution to the pressure is more subtle, due to the possible existence of anisotropies. One way to overcome such difficulties is to use the concept of the

chaotic magnetic field, as originally introduced by Zeldovich in the 1960s: “*It is possible to describe the effect of the magnetic field by using the pressure concept only when we are dealing with a small-scale chaotic field (pag. 158)*” [18]. So, we relax the condition of a uniform magnetic field in the z direction and assume the chaotic magnetic field, whose stress tensor reads: $\text{diag}(B^2/6, B^2/6, B^2/6)$, thus avoiding the anisotropy problem and yielding $p = \epsilon/3$, a radiation pressure formalism. Within the chaotic magnetic field formalism, the EOS reads [19–24]:

$$\epsilon = \epsilon_M + \frac{B^2}{2}, \quad \text{and} \quad p = p_M + \frac{B^2}{6}, \quad (5)$$

where M stands for matter.

Concerning the strength of the magnetic field, powerful magnetars can have a magnetic field around 10^{15} G at their surface [25, 26]. However, due to the scalar Virial theorem [27], the magnetic field at the neutron stars’ core can reach values over 10^{18} G. To simulate the magnetic field growing towards the core, we use an energy density-dependent approach, as done in refs. [19, 24]:

$$B = B_0 \left(\frac{\epsilon_M}{\epsilon_0} \right)^\gamma + B_{\text{surface}}. \quad (6)$$

In this work, we use $B_{\text{surface}} = 10^{12}$ G and $B_0 = 10^{15}$ G for “normal”, weakly magnetized neutron stars and $B_{\text{surface}} = 10^{15}$ G and $B_0 = 3.1 \times 10^{18}$ G for strongly magnetized neutron stars. As pointed out in ref. [20], values of B_0 lower than 10^{17} G do not affect the main properties of neutron stars.

III. EQUATION OF STATE OF MAGNETIZED MATTER

Here, we follow ref. [28] and use the $\text{L}3\omega\rho$ parametrization to fix all the coupling constants of the Lagrangian, except $(g_{N\rho}/m_\rho)^2$ and $\Lambda_{\omega\rho}$, which are fixed to reproduce different values of the slope. As pointed out in ref. [5], the $\text{L}3\omega\rho$ parametrization satisfies the five well-known constraints from nuclear physics. The parameters of the model, the calculated physical quantities, and the respective constraints are presented in Tab. I. In the same context, different values of the slope L obtained by varying $(g_{N\rho}/m_\rho)^2$ and $\Lambda_{\omega\rho}$ are presented in Tab. II.

Parameters	Constraints	This model
$(g_\sigma/m_s)^2$	$n_0(\text{fm}^{-3})$	0.148 - 0.170
$(g_\omega/m_v)^2$	M^*/M	0.6 - 0.8
κ	$K(\text{MeV})$	220.0 - 260.0
λ	$S_0(\text{MeV})$	30.0 - 35.0
--	$B/A(\text{MeV})$	15.8 - 16.5
--		16.2

TABLE I: Model parameters used in this study and their predictions for symmetric nuclear matter at saturation density. The parametrization was taken from ref. [28], and the phenomenological constraints were taken from refs. [6, 7].

L (MeV)	$(g_\rho/m_\rho)^2$ (fm 2)	$\Lambda_{\omega\rho}$ (fm 2)
44.0	8.40	0.0515
60.0	6.16	0.0344
76.0	4.90	0.0171
92.0	4.06	0

TABLE II: Model parameters selected to set the symmetry energy at $S_0 = 31.7$ MeV taken from ref. [28].

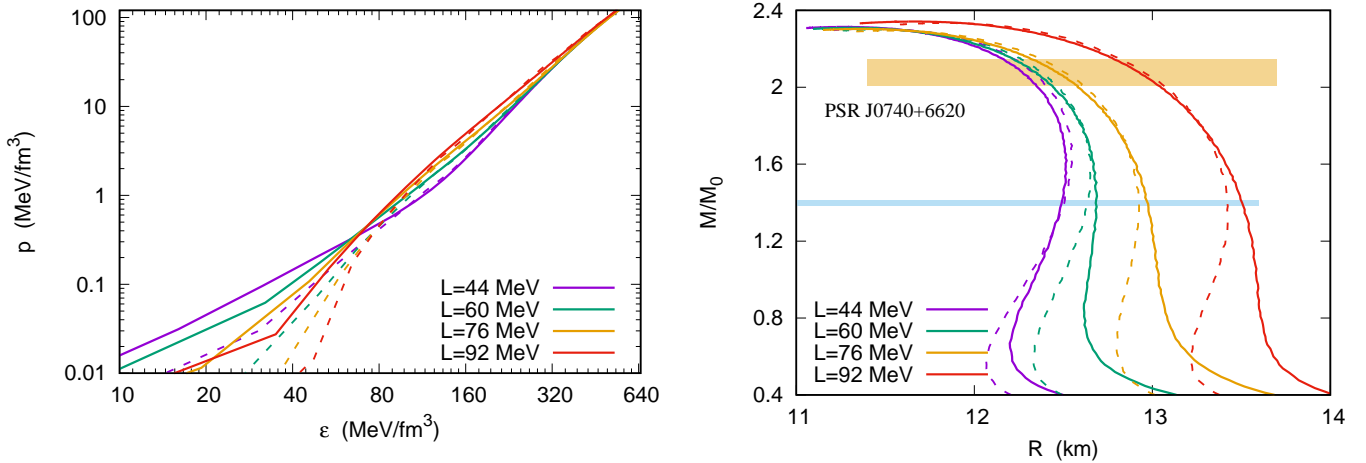


FIG. 1: (left) EOS and (right) mass-radius relation for magnetized matter. Solid lines indicate weakly-magnetized neutron stars, and dotted lines indicate strongly-magnetized ones.

We begin our discussion with the EOS and the corresponding TOV solutions. As already pointed out in the literature, the magnetic field [19] and the slope [28] affect low-mass stars more than massive ones.

In the left panel of Fig. 1, we display the EOS for different values of L with (dashed lines) and without (solid lines) a magnetic field. The effect of the slope and the magnetic field is barely visible on the EOS in a linear scale. Therefore, we display the EOS on a logarithmic scale. We can notice that by changing L , we obtain softer EOS at very low densities ($\epsilon < 80$ MeV/fm 3) for larger values of L . At low-to-moderate density, this effect is inverted, and at high densities, all EOSs become almost degenerate, as discussed in ref. [28]. The same principle applies to the magnetic field. The magnetic field makes the EOS significantly soft at low densities. At larger densities, the EOSs become slightly stiffer due to the magnetic field. The important feature here is that the magnetic field appears to affect more EOSs with higher values of L .

IV. STELLAR STRUCTURE

Since no anisotropies are present, the chaotic magnetic field allows us to use the standard Tolman-Oppenheimer-Volkoff (TOV) equations [29], which represent the hydrostatic equilibrium of the star. In the following lines we will give an explanation of the physical considerations to obtain these equations.

Assuming that the unperturbed compact star is totally composed of a perfect fluid, the stress-energy momentum tensor can be expressed as

$$T_{\mu\nu} = (\epsilon + p)u_\mu u_\nu + pg_{\mu\nu}, \quad (7)$$

and the generic background space-time of a static spherical star is expressed through the line element

$$ds^2 = -e^{\nu(r)}dt^2 + e^{\lambda(r)}dr^2 + r^2(d\theta^2 + \sin^2\theta d\phi^2). \quad (8)$$

where t, r, θ, ϕ are the set of Schwarzschild-like coordinates, and the metric potentials $\nu(r)$ and $\lambda(r)$ are functions of the radial coordinate r only.

The Einstein equations in such a spacetime lead to the following set of stellar structure equations (Tolman-Oppenheimer-Volkoff equations)

$$\frac{dp}{dr} = -\frac{\epsilon(p)m}{r^2} \left(1 + \frac{p}{\epsilon(p)}\right) \left(1 + \frac{4\pi pr^3}{m}\right) \left(1 - \frac{2m}{r}\right)^{-1}, \quad (9)$$

$$\frac{d\nu}{dr} = -\frac{2}{\epsilon(p)} \frac{dp}{dr} \left(1 + \frac{p}{\epsilon(p)}\right)^{-1}, \quad (10)$$

$$\frac{dm}{dr} = 4\pi r^2 \epsilon(p), \quad (11)$$

To close this system we need a relation between the pressure and energy density, which is given by the equation of state $\epsilon(p)$.

Therefore, given an EOS, and by integrating these equations, we can obtain the behavior of the following functions inside the star: $m(r), p(r), \epsilon(r)$ and $\nu(r)$. There is an additional condition in order to consistently determine the $\nu(r)$ function inside the star, it read as

$$\nu(r = R) = \ln \left(1 - \frac{2M}{R} \right), \quad (12)$$

where R is the radius of the star and M its mass. We can determine the stellar structure, once the previously commented functions have been calculated

In the right panel of Fig. 1, we display the stellar masses M vs the radii R , for different values of L with (dashed lines) and without (solid lines) a magnetic field. In all cases, we use the BPS+BPP [30, 31] EOS to simulate the neutron star crust, as suggested in ref. [32], and discussed in ref. [13, 28, 33, 34]. Altogether with the TOV solutions, we also display two constraints. Today, the most well-measured massive pulsar is the PSR J0740+6620, with a mass of $2.08 \pm 0.07 M_{\odot}$ and a radius in the range of $11.41 \text{ km} < R < 13.69 \text{ km}$ [8, 9]. Any realistic EOS must be able to fulfill this constraint, which is presented as a yellowish hatched area. The second constraint is related to the radius of the canonical $1.4 M_{\odot}$ star. Since it is strongly related to the slope [35], we use here only a moderate-to-weak constraint presented in ref. [36]. Using state-of-the-art theoretical results at low and high baryon densities, the authors constrain the radius of the canonical star to $R_{1.4} < 13.6 \text{ km}$. Such a constraint is presented as a bluish hatched area. As can be seen, in this present study, all results fulfill both constraints. There are, nevertheless, strong constraints related to the canonical $1.4 M_{\odot}$ star. For instance, in ref. [9] an upper limit of 13.1 km was appointed.

We now analyze how the strong magnetic field affects the main properties of neutron stars with different masses and slopes. From $1.0 M_{\odot}$ to $2.0 M_{\odot}$, the results for all parameters discussed in this work are presented in Tab. III. Weakly-magnetized neutron stars with $B_0 = 10^{15} \text{ G}$ are referred to as $B0$, while strongly magnetized ones, with $B_0 = 3.1 \times 10^{18} \text{ G}$, are referred to as $B1$.

At first, we can notice that as the slope increases, the radii also increase for all masses. Such an effect was already noted in refs. [28, 33, 35], and we can see that it is also true in the presence of the chaotic magnetic field. Furthermore, for lower masses, strongly magnetized stars present a lower radius than weakly magnetized ones. As the masses increase, the radii become closer, and at some point, strongly magnetized neutron stars present slightly larger radii than weakly magnetized ones. Such an effect exists for all values of the slope L . The mass where the behavior of the radius is inverted depends on the slope. For $L = 44 \text{ MeV}$, a $1.4 M_{\odot}$ strongly magnetized star already has a larger radius than a weakly magnetized one, while for $L = 92 \text{ MeV}$, such an effect only takes place for stars above $1.8 M_{\odot}$.

The effect of a strong magnetic field is more pronounced for higher values of L , as well as for lower masses. Quantitatively, we can notice that for a $1.0 M_{\odot}$, the difference in the radius, ΔR , can reach 0.24 km for $L = 92 \text{ MeV}$, or only 0.06 km for $L = 44 \text{ MeV}$. Higher mass stars are affected by a $\Delta R < 0.1 \text{ km}$ for all values of L . All relevant values are presented in Tab. III. As pointed out, both observational constraints are fulfilled by all values of L and B_0 .

Another relevant physical quantity that can be obtained from the computations of the stellar structure is the gravitational redshift Z . The gravitational redshift is defined as [37]:

$$Z = \left(1 - \frac{2M}{R} \right)^{-1/2} - 1. \quad (13)$$

The results for masses in the range $0.4 M_{\odot} < M < 2.0 M_{\odot}$ are displayed on the top-left side of Fig. 2, while a zoomed version is displayed at the bottom-left in the same figure. We can notice that as the mass increases, the redshift also increases, independently of the value of L or B_0 . We can also see that the redshift is strongly dependent on the slope L , but the effects of the magnetic field are small. In the case of the slope, we can see that small slopes can produce values of Z about 0.115 larger than high values of L . On the other hand, the presence of a strong magnetic field causes only a $\Delta Z < 0.005$ in all cases. The values of Z and ΔZ for some masses are presented in Tab. III. Our results indicate that measuring the redshift can be a useful tool for constraining the slope, but not the strength, of the magnetic field.

V. TIDAL DEFORMABILITY

After the computation of the equilibrium configuration we proceed to the study of tidal deformations, which depend on the internal structure of neutron stars and our purpose is to use it as an additional constraint for the equation of state

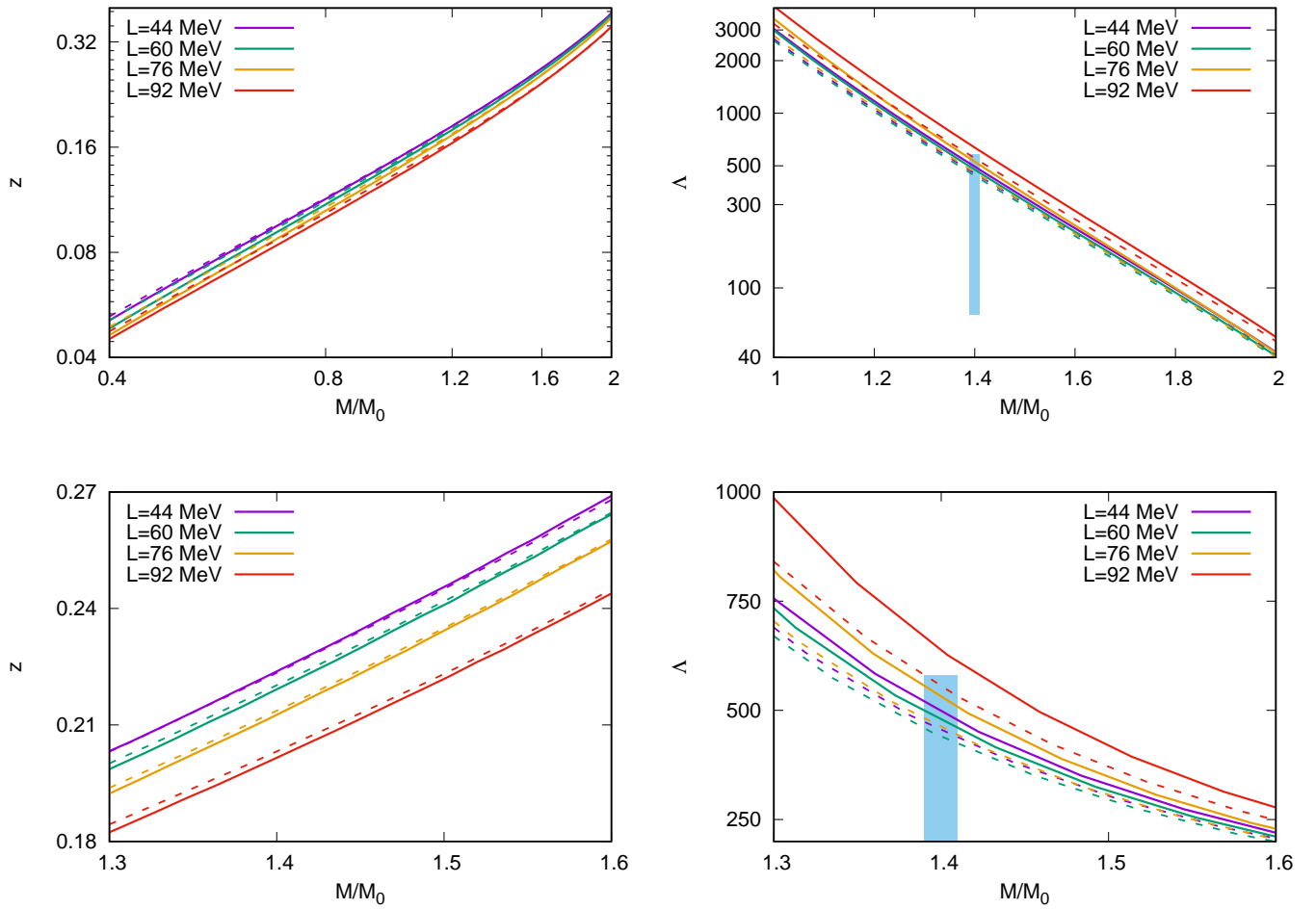


FIG. 2: (Top-left) Redshift and (Top-right) dimensionless tidal parameter. (Bottom) Zoom-in focusing on masses between 1.3 and 1.6 solar masses. Solid lines indicate weakly-magnetized neutron stars, and dotted lines indicate strongly-magnetized ones.

of magnetars. For this objective we present, in the next lines, some comments about the theory of tidal deformabilities, the main equations and relationships that are necessary for our work.

The relativistic theory of tidal effects was deduced by Damour and Nagar, Binnington and Poisson [38, 39]. They concluded that the tidal deformation of a neutron star is characterized by the gravito-electric K_2^{el} and gravito-magnetic K_2^{mag} Love numbers, where the former is related to the mass quadrupole and the second to the current quadrupole induced by the companion star. Further researches by Flanagan and Hindeler concluded that only a single detection should be sufficient to impose upper limits on K_2^{el} at 90% confidence level [40]. Since then intense research has been invested on the computing of Love numbers of neutron stars [41–45].

In a binary system the induced quadrupole moment Q_{ij} in one neutron star due to the external tidal field \mathcal{E}_{ij} created by a companion compact object can be written as [44, 45],

$$Q_{ij} = -\lambda \mathcal{E}_{ij}, \quad (14)$$

where, λ is the tidal deformability parameter, which can be expressed in terms of dimensionless $l = 2$ quadrupole tidal Love number k_2 as

$$\lambda = \frac{2}{3} k_2 R^5. \quad (15)$$

To obtain k_2 we have to solve the following differential equation

$$r \frac{dy}{dr} + y^2 + yF(r) + r^2 Q(r) = 0, \quad (16)$$

where the coefficients are given by

$$F(r) = [1 - 4\pi r^2(\varepsilon - p)]/E \quad (17)$$

and

$$Q(r) = 4\pi \left[5\varepsilon + 9p + (\varepsilon + p) \left(\frac{\partial p}{\partial \varepsilon} \right)^{-1} - \frac{6}{4\pi r^2} \right] / E - 4 \left[\frac{m + 4\pi r^3 p}{r^2 E} \right]^2, \quad (18)$$

with $E = 1 - 2m/r$, ε and p are the energy density and pressure profiles inside the star. Therefore the Love number k_2 can be obtained as

$$k_2 = \frac{8C^5}{5} (1 - 2C)^2 [2 + C(y_R - 1) - y_R] \times \left\{ 2C[6 - 3y_R + 3C(5y_R - 8)] + 4C^3[13 - 11y_R + C(3y_R - 2) + 2C^2(1 + y_R)] + 3(1 - 2C^2)[2 - y_R + 2C(y_R - 1)] \ln(1 - 2C) \right\}^{-1}, \quad (19)$$

where $y_R = y(r = R)$ and $C = M/R$ are the star compactness, M and R are the total mass and radius of the star, respectively. Equation (16) has to be solved coupled to the TOV equations. The dimensionless tidal parameter is defined as:

$$\Lambda = \frac{2k_2}{3C^5}, \quad (20)$$

Adicional discussion can be found in ref. [20, 45–47] and the references therein. The numerical results are presented on the Top-right side of Fig. 2, while in the bottom-right we present a zoomed version focusing on masses between 1.3 and $1.6M_\odot$. The observational constraint coming from the GW170817 event detected by LIGO/VIRGO gravitational wave observatories is also presented as a bluish hatched area. It was pointed out in ref. [10] that the tidal dimensionless parameter of the canonical star must lie in the range $70 < \Lambda_{1.4} < 580$. As shown, this constraint is satisfied for almost all values of L and B_0 investigated in the present work. The only exception is $L = 92$ MeV within the weak-magnetic-field limit.

The presence of the magnetic field always decreases the tidal parameter Λ . This is valid for all slopes and all masses. Moreover, a strong magnetic field can affect the tidal parameter even more than a change in the slope. For instance, in the case of the canonical star, we see that the lower value of the slope is obtained for $L = 60$ MeV, which within the weak magnetic field, assumes $\Lambda_{1.4} = 501$. However, within the strong magnetic field, values lower than 500 can be obtained for $L = 44$ MeV and $L = 76$ MeV as well. This indicates that the tidal parameter is more dependent on the EOS at the low-density limit than the mass-radius relation.

In relation to other mass values, we can see that the effect of the magnetic field is, as expected, stronger for low masses. In the same sense, the effects are larger for larger values of L . Moreover, for massive neutron stars, the dimensionless tidal parameter seems almost independent of both the slope and the magnetic field. Regarding these features, we can notice that $\Delta\Lambda$ can reach absolute values above 800 for $1.0 M_\odot$. This corresponds to variations up to almost 20%. We can conclude that for all physical quantities analysed till this moment, the tidal parameter presents the largest sensitivity to the effects of a strong magnetic field. The results for Λ and $\Delta\Lambda$ for different masses can be found in Tab. III.

VI. NEUTRON STAR OSCILLATIONS

The equations governing the nonradial pulsations of a compact star in full general relativity were first investigated by Thorne and Campolattaro [48, 49]. They demonstrated that Einstein's equations for small, nonradial, quasi-periodic oscillations of relativistic stellar models can be reduced to a system of ordinary differential equations for the perturbed variables. In this work, we adopt the formulation developed by Lindblom and Detweiler [50, 51], in which Thorne's perturbation equations are reduced to a system of four ordinary differential equations, allowing the perturbations to

be integrated directly in a manner similar to Thorne's original approach. These equations describe both the fluid oscillations of the star and the associated emission of gravitational waves, which in turn leads to damping of the stellar oscillations.

We assume that the unperturbed, spherically symmetric equilibrium configuration of the compact star is described by a solution of the Tolman–Oppenheimer–Volkoff (TOV) equations and then we consider perturbations in the fluid and metric. For pulsations with spherical-harmonic indices ℓ and m and with parity $\pi = (-1)^\ell$, the perturbed metric inside the star, expressed in the Regge–Wheeler gauge [52] takes the form

$$ds^2 = -e^\nu(1 + r^\ell H_0^{\ell m} Y_{\ell m} e^{i\omega t}) dt^2 + e^\lambda(1 - r^\ell H_2^{\ell m} Y_{\ell m} e^{i\omega t}) dr^2 - 2i\omega r^{\ell+1} H_1^{\ell m} Y_{\ell m} e^{i\omega t} dt dr + r^2(1 - r^\ell K^{\ell m} Y_{\ell m} e^{i\omega t})(d\theta^2 + \sin^2 \theta d\varphi^2), \quad (21)$$

where ω is the frequency, $Y_{\ell m}$ denote the usual scalar spherical harmonics, the functions e^ν and e^λ are the components of the metric of the unperturbed stellar model, while $H_i^{\ell m}(r)$ and $K^{\ell m}(r)$ characterize the metric perturbations. The fluid perturbation is described by the Lagrangian displacement vector ξ_a , having components

$$\begin{aligned} \xi_r(t, r, \theta, \varphi) &= e^{\lambda/2} r^{\ell-1} W^{\ell m}(r) Y_{\ell m}(\theta, \varphi) e^{i\omega t}, \\ \xi_\theta(t, r, \theta, \varphi) &= -r^\ell V^{\ell m}(r) \partial_\theta Y_{\ell m}(\theta, \varphi) e^{i\omega t}, \\ \xi_\varphi(t, r, \theta, \varphi) &= -r^\ell V^{\ell m}(r) \partial_\varphi Y_{\ell m}(\theta, \varphi) e^{i\omega t}. \end{aligned} \quad (22)$$

In the present paper we use the formulation of Lindblom and Detweiler [50, 51], consisting of a system of four ordinary differential equations, as given in [53]:

$$\frac{d\mathbf{Y}(r)}{dr} = \mathbf{Q}(r, \ell, \omega) \mathbf{Y}(r) \quad (23)$$

for the functions $\mathbf{Y}(r) = (H_1^{\ell m}, K^{\ell m}, W^{\ell m}, X^{\ell m})$, where

$$X^{\ell m} = -e^{\psi/2} \Delta p^{\ell m} \quad (24)$$

and three algebraic relations, which allow us to compute the remaining functions $\{H_0^{\ell m}, H_2^{\ell m}, V^{\ell m}\}$ in terms of the others. We concentrate our attention on normal modes that belong to a particular even parity spherical harmonic $\pi = (-1)^\ell$ with the complex frequency [53]

$$\omega = \sigma + \frac{i}{\tau}. \quad (25)$$

The normal modes of the coupled system are defined as those oscillations that lead to purely outgoing waves at spatial infinity. The real parts of ω correspond to the oscillatory frequency

$$f = Re(\omega)/2\pi = \sigma/2\pi \quad (26)$$

and the damping time,

$$\tau = 1/Im(\omega), \quad (27)$$

which is related to the imaginary part of ω and corresponds to the radiative energy loss emitted through gravitational waves.

The fundamental mode (*f*-mode) corresponds to a class of non-radial oscillation modes in compact stars and is primarily determined by the global properties of the star, such as its mass and radius. These oscillations act as sources of gravitational waves, whose characteristic frequencies and damping times are highly sensitive to the EoS of the stellar interior. As a result, the *f*-mode serves as a powerful diagnostic tool for probing the internal structure and composition of neutron stars.

We can see that, for low masses $M < 1.4M_\odot$ and by increasing L , we obtain a decreasing of the gravitational wave frequencies, all below $f < 1.7\text{kHz}$. For masses higher than $1.4M_\odot$ the effect is almost insignificant and all the frequencies converges to approximately $f < 2.1\text{kHz}$. In the case of a strong magnetic field (dashed lines), for masses below $M < 2.0M_\odot$, the frequencies have a systematic shifting and the the difference is about 1.8 %, but for masses above $2.0M_\odot$ the magnetic field has not significant effect. A similar behaviour is observed for the damping time. In fact, for massive stars, the damping time converges to 150 ms. We can conclude that the magnetic field does not have a significant effect on massive stars, but higher values of L have a considerable effect.

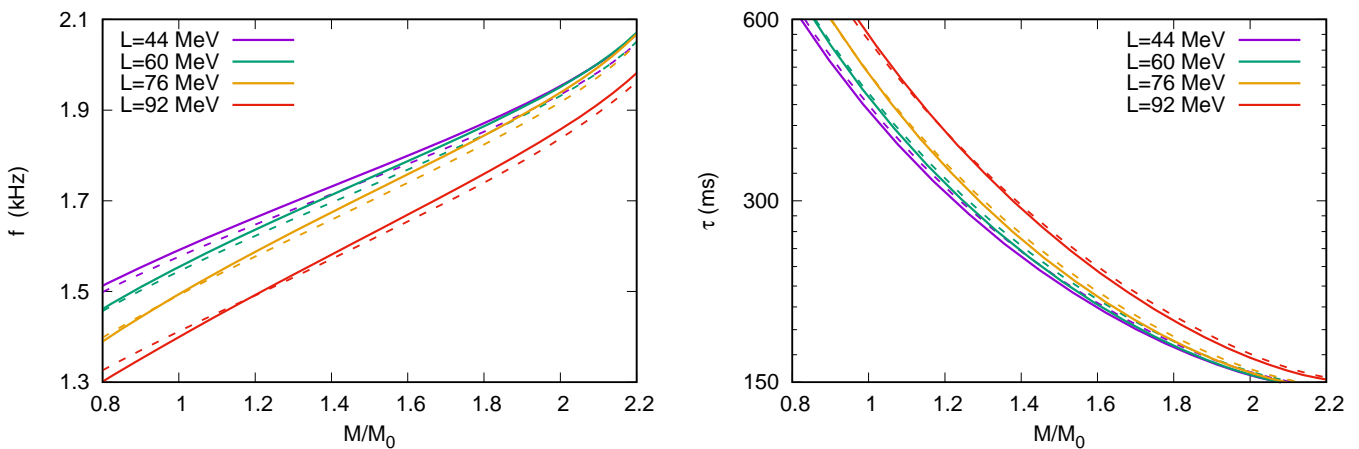


FIG. 3: **left)** Frequency of the fundamental mode **(right)** damping time. Solid lines indicate weakly-magnetized neutron stars, and dotted lines indicate strongly-magnetized ones

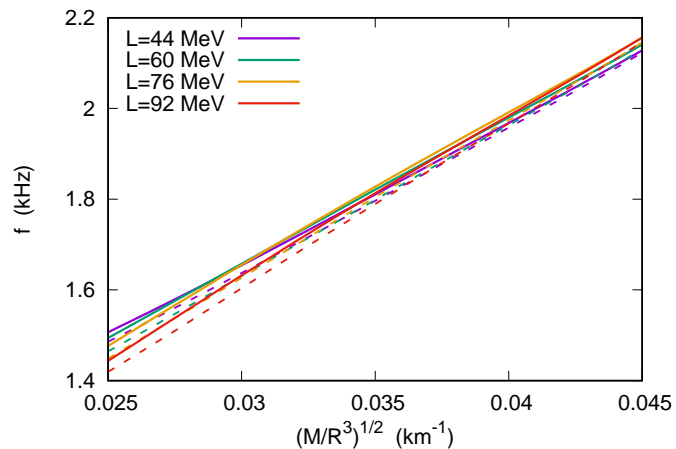


FIG. 4: The frequency of the fundamental mode is plotted in the upper panel as a function of the square root of the average density for the different EoSs. Solid lines indicate weakly-magnetized neutron stars, and dotted lines indicate strongly-magnetized ones

Before finishing our analyses, we have investigated the universal relation between the frequency of the fundamental mode and the square root of the average density, $(M/R^3)^{1/2}$. It was pointed out in Ref. [54] that in the Newtonian limit of the theory of stellar perturbations, the frequency scales as the square root of the average density; and the gravitational wave frequency can be fitted by the following linear expression:

$$f = a + b \cdot (M/R^3)^{1/2}, \quad (28)$$

where a is given in kHz and b in $\text{km} \times \text{kHz}$. These results are displayed in Fig. 4 for masses above $0.65 M_\odot$, and the calculated values of a and b are presented in Tab. IV altogether with some values that can be found in the literature.

We notice that, as a general rule, as we increase the value of L we reduce the value of a and increase the value of b . A deviation of this rule is the value of $L = 60$ MeV. As happens with the dimensionless tidal parameter, this value of L predicts the lower value of b for all analyzed slopes. A strong magnetic field also acts to decrease the value of a and increase the value of b . We found a median value of $a = 0.611$ kHz and $b = 34.1$ $\text{km} \times \text{kHz}$ for the weak magnetic field approach (very similar to the values found in ref. [55]); and $a = 0.550$, $b = 35.3$ $\text{km} \times \text{kHz}$ for the strong magnetic field.

L (MeV)	B_0	M (M_\odot)	R (km)	ΔR (km)	Λ	$\Delta\Lambda$	z	Δz	f (kHz)	Δf (kHz)	τ (ms)	$\Delta\tau$ (ms)	ϵ_c (MeV/fm ³)
44	B0	1.0	12.34	-	3026	-	0.146	-	1.592	-	424	-	330
44	B1	1.0	12.28	-0.06	2695	-331	0.147	+0.001	1.574	-0.018	434	+10	323
44	B0	1.2	12.43	-	1200	-	0.183	-	1.667	-	310	-	368
44	B1	1.2	12.40	-0.03	1066	-134	0.183	0.000	1.648	-0.019	317	+7	359
44	B0	1.4	12.51	-	506	-	0.224	-	1.734	-	243	-	406
44	B1	1.4	12.52	+0.01	475	-31	0.224	0.000	1.714	-0.020	258	+5	397
44	B0	1.6	12.51	-	226	-	0.269	-	1.801	-	200	-	456
44	B1	1.6	12.55	+0.04	209	-17	0.268	-0.001	1.782	-0.019	204	+4	447
44	B0	2.0	12.35	-	45	-	0.388	-	1.954	-	154	-	602
44	B1	2.0	12.41	+0.06	42	-3	0.384	-0.004	1.936	-0.018	156	+2	589
60	B0	1.0	12.65	-	3011	-	0.143	-	1.558	-	448	-	326
60	B1	1.0	12.49	-0.16	2619	-392	0.145	+0.002	1.547	-0.011	455	+7	319
60	B0	1.2	12.66	-	1154	-	0.178	-	1.638	-	322	-	364
60	B1	1.2	12.57	-0.09	1042	-112	0.180	+0.002	1.624	-0.014	328	+6	355
60	B0	1.4	12.71	-	501	-	0.220	-	1.714	-	248	-	405
60	B1	1.4	12.66	-0.05	460	-41	0.221	+0.001	1.696	-0.018	253	+5	395
60	B0	1.6	12.68	-	213	-	0.267	-	1.788	-	202	-	455
60	B1	1.6	12.66	-0.02	201	-12	0.267	0.000	1.770	-0.018	206	+4	446
60	B0	2.0	12.44	-	42	-	0.384	-	1.951	-	154	-	605
60	B1	2.0	12.47	+0.03	40	-2	0.382	-0.002	1.933	-0.018	156	+2	593
76	B0	1.0	13.04	-	3501	-	0.138	-	1.495	-	488	-	314
76	B1	1.0	12.87	-0.17	2807	-694	0.140	+0.002	1.495	0.000	488	0	306
76	B0	1.2	13.00	-	1307	-	0.173	-	1.589	-	342	-	355
76	B1	1.2	12.90	-0.10	1099	-208	0.175	+0.002	1.578	-0.011	347	+5	346
76	B0	1.4	12.99	-	535	-	0.213	-	1.677	-	260	-	399
76	B1	1.4	12.93	-0.06	482	-53	0.214	+0.001	1.659	-0.018	265	+5	390
76	B0	1.6	12.91	-	236	-	0.258	-	1.759	-	208	-	451
76	B1	1.6	12.89	-0.02	208	-18	0.258	0.000	1.740	-0.019	212	+4	441
76	B0	2.0	12.58	-	43	-	0.376	-	1.939	-	156	-	606
76	B1	2.0	12.61	+0.03	41	-2	0.374	-0.002	1.919	-0.020	158	+2	594
92	B0	1.0	13.59	-	4111	-	0.131	-	1.400	-	566	-	278
92	B1	1.0	13.35	-0.24	3306	-805	0.134	+0.003	1.415	+0.015	55	-11	272
92	B0	1.2	13.56	-	1555	-	0.164	-	1.493	-	388	-	319
92	B1	1.2	13.40	-0.16	1307	-248	0.167	+0.003	1.493	0.000	388	0	310
92	B0	1.4	13.49	-	640	-	0.202	-	1.582	-	292	-	363
92	B1	1.4	13.41	-0.08	566	-74	0.203	+0.001	1.571	-0.011	295	+3	355
92	B0	1.6	13.41	-	287	-	0.244	-	1.670	-	229	-	416
92	B1	1.6	13.37	-0.04	251	-36	0.245	+0.001	1.655	-0.015	233	+4	404
92	B0	2.0	13.05	-	55	-	0.354	-	1.857	-	165	-	560
92	B1	2.0	13.07	+0.02	51	-4	0.353	-0.001	1.838	-0.019	167	+2	548

TABLE III: Neutron stars' main properties for different values of L with weak and strong magnetic field.

There are several promising avenues for measuring f-mode [56–58] characteristics in compact stars. For instance, third-generation gravitational wave detectors like the Einstein Telescope [59] and Cosmic Explorer [60] are expected to achieve the sensitivity required for detecting f-mode signals from astrophysical sources [61].

VII. CONCLUSIONS

In this work, we studied the effects of a strong magnetic field for different values of the symmetry energy slope. The main results can be summarized as:

- At very low density, larger slope values produce soft EOS. This is reversed at low and moderate densities. In the high-density limit, all EOS become almost degenerate.
- Strongly magnetized EOS are soft at low densities but stiffer at moderate densities. The effect is more significant for higher values of the slope.

L (MeV)	B_0	a	b
44	B0	0.652	32.8
44	B1	0.450	37.2
60	B0	0.691	32.2
60	B1	0.633	33.3
76	B0	0.616	34.2
76	B1	0.587	34.6
92	B0	0.485	37.2
92	B1	0.530	35.9
Mean	B0	0.611	34.1
Mean	B1	0.550	35.3
Other works	Ref.		
Anderson et al.	Ref. [62]	0.220	47.5
Pradhan et al.	Ref. [63]	0.790	33.0
Benhar et al.	Ref. [54]	0.535	36.2
Guha Roy et al.	Ref. [55]	0.626	35.9
Chirenti et al.	Ref. [64]	0.332	44.0

TABLE IV: Values of fitting coefficients for Eq. 28 from different values of L and magnetic field. Results presented in other works are also added.

- For a fixed mass, the neutron star radius grows with L . In the case of the magnetic field, we see that low mass stars bear lower radii, but high mass stars actually present larger values of R . The mass for which the radii are the same for weakly and strongly magnetized neutron stars depends on L . For $L = 44$ MeV, this mass lies below $1.4 M_\odot$. On the other hand, for $L = 92$ MeV, $M > 1.8 M_\odot$.
- All models discussed in this work satisfy the constraints related to the PSR J0740+6620 and the radius of the canonical star.
- The gravitational redshift is sensitive to the slope, but not to the strong magnetic fields. In all cases, strong magnetic fields only produce absolute values of $\Delta z < 0.005$.
- In contrast to the redshift, the tidal dimensionless parameter is very sensitive to the magnetic field. Within the weak magnetic field limit, we always obtain $\Lambda_{1.4} > 500$. But, for the strong magnetic field, $\Lambda < 500$ for three different values of L . In the lower mass limit, a strong magnetic field can produce an absolute value of $\Delta\Lambda > 800$.
- We have seen that, in the case of the gravitational wave frequency, the magnetic field has a tiny effect on masses below $2.0 M_\odot$.
- Our results show that an increase in L , in the region of low masses, produces a decrease in the gravitational wave frequencies. In the case of large masses, L does not produce any effect.
- By analysing the universal relation of Eq. 28, we see that an increase of the slope causes a decrease in a but an increase in b . The same happens when we increase the strength of the magnetic field.

Acknowledgments

This work is a part of the project INCT-FNA proc. No. 408419/2024-5. It is also supported by Conselho Nacional de Desenvolvimento Científico e Tecnológico (CNPq) under Grants No. 303490/2021-7 (D.P.M.), 305347/2024-1 (L.L.L.) and 304569/2022-4 (C.V.F.).

[1] C. Thompson and R. C. Duncan, “The soft gamma repeaters as very strongly magnetized neutron stars - I. Radiative mechanism for outbursts,” *mnras*, vol. 275, pp. 255–300, July 1995.

- [2] S. Mereghetti, J. Pons, and A. Melatos, "Magnetars: Properties, Origin and Evolution," *Space Sci. Rev.*, vol. 191, no. 1-4, pp. 315–338, 2015.
- [3] S. A. Olausen and V. M. Kaspi, "The McGill Magnetar Catalog," *Astrophys. J. Suppl.*, vol. 212, p. 6, 2014.
- [4] B. D. Serot, "Quantum hadrodynamics," *Rep. Progr. Phys.*, vol. 55, pp. 1855–1946, nov 1992.
- [5] L. L. Lopes, "Hyperonic neutron stars: reconciliation between nuclear properties and nicer and ligo/virgo results," *Commun. Theor. Phys.*, vol. 74, p. 015302, dec 2022.
- [6] M. Dutra, O. Lourenço, S. S. Avancini, *et al.*, "Relativistic mean-field hadronic models under nuclear matter constraints," *Phys. Rev. C*, vol. 90, p. 055203, Nov 2014.
- [7] M. Oertel, M. Hempel, T. Klähn, and S. Typel, "Equations of state for supernovae and compact stars," *Rev. Mod. Phys.*, vol. 89, p. 015007, Mar 2017.
- [8] T. Riley *et al.*, "A NICER View of the Massive Pulsar PSR J0740+6620 Informed by Radio Timing and XMM-Newton Spectroscopy," *Astrophys. J. Lett.*, vol. 918, p. L27, sep 2021.
- [9] M. Miller *et al.*, "The Radius of PSR J0740+6620 from NICER and XMM-Newton Data," *Astrophys. J. Lett.*, vol. 918, p. L28, sep 2021.
- [10] B. P. Abbott, R. Abbott, T. D. Abbott, *et al.*, "Gw170817: Measurements of neutron star radii and equation of state," *Phys. Rev. Lett.*, vol. 121, p. 161101, 2018.
- [11] F. Fattoyev *et al.*, "Relativistic effective interaction for nuclei, giant resonances, and neutron stars," *Phys. Rev. C*, vol. 82, p. 055803, 2010.
- [12] L. Lopes and D. Menezes, "The influence of hyperons and strong magnetic field in neutron star properties," *Braz. J. Phys.*, vol. 42, p. 428, 2012.
- [13] L. L. Lopes, "An undergraduate approach to the quantum hadrodynamics and physics of neutron stars," *Universe*, vol. 11, no. 8, 2025.
- [14] J. Boguta and A. Bodmer, "Relativistic calculation of nuclear matter and the nuclear surface," *Nucl. Phys. A*, vol. 292, p. 413, 1977.
- [15] Q.-h. Peng and H. Tong, "The physics of strong magnetic fields in neutron stars," *Mon. Not. Roy. Astron. Soc.*, vol. 378, pp. 159–162, 2007.
- [16] A. Broderick, M. Prakash, and J. M. Lattimer, "The equation of state of neutron star matter in strong magnetic fields," *Astrophys. J.*, vol. 537, p. 351, 2000.
- [17] A. Rabhi, H. Pais, P. K. Panda, and C. Providência, "Quark–hadron phase transition in a neutron star under strong magnetic fields," *J. Phys. G*, vol. 36, p. 115204, 2009.
- [18] Y. B. Zel'dovich and I. Nivikov, *Compact stars*.: Dover, New York, 1996.
- [19] L. Lopes and D. Menezes, "On magnetized neutron stars," *J. Cosm. Astrop. Phys.*, vol. 2015, no. 08, p. 002, 2015.
- [20] C. Flores, L. Lopes, L. Benito, and D. Menezes, "Gravitational wave signatures of highly magnetized neutron stars," *Eur. Phys. J. C*, vol. 80, p. 1142, 2020.
- [21] L. L. Lopes and D. P. Menezes, "Role of vector channel in different classes of (non) magnetized neutron stars," *Eur. Phys. J. A*, vol. 56, p. 122, 2020.
- [22] F. Wu, C. Wu, and Z.-Z. Ren, "Neutron stars including the effects of chaotic magnetic fields and anomalous magnetic moments*," *Chin. Phys. C*, vol. 41, p. 045102, 2017.
- [23] M. Pelicer and D. Menezes, "Phase transitions and latent heat in magnetized matter," *Eur. Phys. J. A*, vol. 58, p. 177, 2022.
- [24] M. Lawrence Pattersons *et al.*, "Rotating neutron stars with chaotic magnetic fields in general relativity and rastall gravity," *Inter. J. Mod. Phys. D*, vol. 34, p. 2550074, 2025.
- [25] C. Thompson and R. C. Duncan, "The soft gamma repeaters as very strongly magnetized neutron stars - i. radiative mechanism for outbursts," *Mon. Not. Roy. Astron. Soc.*, vol. 275, pp. 255–300, 1995.
- [26] C. Thompson and R. C. Duncan, "The soft gamma repeaters as very strongly magnetized neutron stars. ii. quiescent neutrino, x-ray, and alfvén wave emission," *Astrophys. J.*, vol. 473, p. 322, 1996.
- [27] S. L. Shapiro and S. A. Teukolsk, *Black Holes, White Dwarf and Neutron Stars*. Wiley, New York, 1983.
- [28] L. L. Lopes *et al.*, "Imprints of the nuclear symmetry energy slope in gravitational wave signals emanating from neutron stars," *Phys. Rev. D*, vol. 108, p. 083042, Oct 2023.
- [29] J. R. Oppenheimer and G. M. Volkoff, "On massive neutron cores," *Phys. Rev.*, vol. 55, pp. 374–381, Feb 1939.
- [30] G. Baym, C. Pethick, and P. Sutherland, "The ground state of matter at high densities," *Astrophys. J.*, vol. 170, p. 299, 1971.
- [31] G. Baym, H. A. Bethe, and C. J. Pethick, "Neutron star matter," *Nucl. Phys. A*, vol. 175, no. 2, p. 225, 1971.
- [32] N. K. Glendenning, *Compact stars*.: 2 ed. Edition, Springer New York, 2000.
- [33] L. L. Lopes, "Role of the symmetry energy slope in neutron stars: Exploring the model dependency," *Phys. Rev. C*, vol. 110, p. 015805, 2024.
- [34] L. L. Lopes, "Decoding rotating neutron stars: Role of the symmetry energy slope," *Astrophys. J.*, vol. 966, p. 184, 2024.
- [35] R. Cavagnoli, D. Menezes, and C. Providencias, "Neutron star properties and the symmetry energy," *Phys. Rev. C*, vol. 84, p. 065810, 2011.
- [36] E. Annala, T. Gorda, A. Kurkela, and A. Vuorinen, "Gravitational-wave constraints on the neutron-star-matter equation of state," *Phys. Rev. Lett.*, vol. 120, p. 172703, 2018.
- [37] L. L. Lopes, "The neutron star inner crust: An empirical essay," *Europhys. Lett.*, vol. 134, p. 52001, 2021.
- [38] T. Damour and A. Nagar, "Relativistic tidal properties of neutron stars," *Phys. Rev. D*, vol. 80, p. 084035, Oct 2009.
- [39] T. Binnington and E. Poisson, "Relativistic theory of tidal love numbers," *Phys. Rev. D*, vol. 80, p. 084018, Oct 2009.

[40] E. E. Flanagan and T. Hinderer, “Constraining neutron-star tidal love numbers with gravitational-wave detectors,” *Phys. Rev. D*, vol. 77, p. 021502, Jan 2008.

[41] F. J. Fattoyev, J. Carvajal, W. G. Newton, and B.-A. Li, “Constraining the high-density behavior of the nuclear symmetry energy with the tidal polarizability of neutron stars,” *Phys. Rev. C*, vol. 87, p. 015806, Jan 2013.

[42] N. Hornick, L. Tolos, A. Zacchi, J.-E. Christian, and J. Schaffner-Bielich, “Relativistic parameterizations of neutron matter and implications for neutron stars,” *Phys. Rev. C*, vol. 98, p. 065804, Dec 2018.

[43] B. Kumar, S. K. Biswal, and S. K. Patra, “Tidal deformability of neutron and hyperon stars within relativistic mean field equations of state,” *Phys. Rev. C*, vol. 95, p. 015801, Jan 2017.

[44] T. Hinderer, B. D. Lackey, R. N. Lang, and J. S. Read, “Tidal deformability of neutron stars with realistic equations of state and their gravitational wave signatures in binary inspiral,” *Phys. Rev. D*, vol. 81, p. 123016, Jun 2010.

[45] T. Hinderer, “Tidal love numbers of neutron stars,” *Astrophys. J.*, vol. 677, p. 1216, apr 2008.

[46] K. Chatzioannou, C.-J. Haster, and A. Zimmerman, “Measuring the neutron star tidal deformability with equation-of-state-independent relations and gravitational waves,” *Phys. Rev. D*, vol. 97, p. 104036, May 2018.

[47] K. Chatzioannou, “Neutron-star tidal deformability and equation-of-state constraints,” *Gen. Rel. Grav.*, vol. 52, p. 109, 2020.

[48] K. S. Thorne and A. Campolattaro, “Non-Radial Pulsation of General-Relativistic Stellar Models. I. Analytic Analysis for $L \geq 2$,” Sept. 1967.

[49] A. Campolattaro and K. S. Thorne, “Nonradial Pulsation of General-Relativistic Stellar Models. V. Analytic Analysis for $L = 1$,” *Astrophys. J.*, vol. 159, p. 847, Mar. 1970.

[50] L. Lindblom and S. L. Detweiler, “The quadrupole oscillations of neutron stars.,” *apjs*, vol. 53, pp. 73–92, Sept. 1983.

[51] S. Detweiler and L. Lindblom, “On the nonradial pulsations of general relativistic stellar models,” *Astrophys. J.*, vol. 292, pp. 12–15, May 1985.

[52] T. Regge and J. A. Wheeler, “Stability of a Schwarzschild Singularity,” *Physical Review*, vol. 108, pp. 1063–1069, Nov. 1957.

[53] C. V. Flores, A. Parisi, C.-S. Chen, and G. Lugones, “Fundamental oscillation modes of self-interacting bosonic dark stars,” *Journal of Cosmology and Astroparticle Physics*, vol. 2019, p. 051, jun 2019.

[54] O. Benhar, V. Ferrari, and L. Gualtieri, “Gravitational wave asteroseismology reexamined,” *Phys. Rev. D*, vol. 70, p. 124015, Dec 2004.

[55] D. Guha Roy, T. Malik, S. Bhattacharya, and S. Banik, “Analysis of neutron star f-mode oscillations in general relativity with spectral representation of nuclear equations of state,” *Astrophys. J.*, vol. 968, p. 124, 2024.

[56] L. Lindblom and B. J. Owen, “Effect of hyperon bulk viscosity on neutron-star r-modes,” *Phys. Rev. D*, vol. 65, p. 063006, Mar 2002.

[57] C. Vásquez Flores and G. Lugones, “Discriminating hadronic and quark stars through gravitational waves of fluid pulsation modes,” *Classical and Quantum Gravity*, vol. 31, p. 155002, jul 2014.

[58] T. Zhao and J. M. Lattimer, “Universal relations for neutron star f-mode and g-mode oscillations,” *Phys. Rev. D*, vol. 106, p. 123002, Dec 2022.

[59] M. Punturo, M. Abernathy, F. Acernese, *et al.*, “The einstein telescope: a third-generation gravitational wave observatory,” *Classical and Quantum Gravity*, vol. 27, p. 194002, sep 2010.

[60] B. P. Abbott, R. Abbott, T. D. Abbott, *et al.*, “Gw170817: Observation of gravitational waves from a binary neutron star inspiral,” *Phys. Rev. Lett.*, vol. 119, p. 161101, Oct 2017.

[61] B. Zink, P. D. Lasky, and K. D. Kokkotas, “Are gravitational waves from giant magnetar flares observable?,” *Phys. Rev. D*, vol. 85, p. 024030, Jan 2012.

[62] N. Andersson and K. D. Kokkotas, “Towards gravitational wave asteroseismology,” *Mon. Not. Roy. Astron. Soc.*, vol. 299, pp. 1059–1068, 10 1998.

[63] B. K. Pradhan, D. Chatterjee, M. Lanoye, and P. Jaikumar, “General relativistic treatment of f-mode oscillations of hyperonic stars,” *Phys. Rev. C*, vol. 106, p. 015805, 2022.

[64] C. Chirenti, G. H. de Souza, and W. Kastaun, “Fundamental oscillation modes of neutron stars: validity of universal relations,” *Phys. Rev. D*, vol. 91, no. 4, p. 044034, 2015.